analytical chemistry

pubs.acs.org/ac Letter

Balanced Detection Method Using Optical Affinity Sensors for Quick Measurement of Biomolecule Concentrations

Yeseul Kim and Hansuek Lee*

Cite This: *Anal. Chem.* 2020, 92, 6189−6193 Read Online

ACCESS | Metrics & More | Article Recommendations

ABSTRACT: To determine the concentration of biomolecules using a label-free optical biosensor, it is necessary to measure the serial signal from the reaction starting point, which is inconvenient for practical applications. Here, we propose an alternative detection method for determining the concentration of a biomolecule. The method, which is derived from the fraction bound equation of the Langmuir adsorption model, determines the concentration relative to a reference sample with required accuracy, with a single measurement at any point in time. We also experimentally demonstrated the method and its accuracy by detecting streptavidin−biotin complexes using on-chip optical sensors based on active disk resonators integrated with microfluidic circuits. By performing the proposed method in a simultaneous parallel measurement scheme, signal fluctuations evenly induced in the detectors by external perturbations could be automatically suppressed, similar to the balanced detection method. We expect our approach to be applicable to practical applications where fast and accurate detection responses are needed.

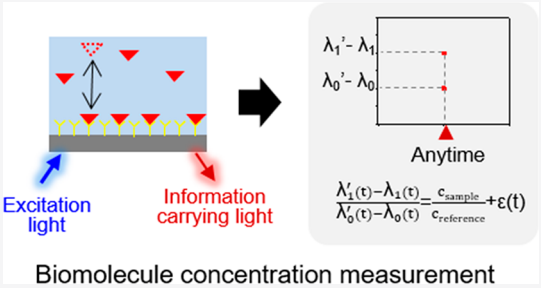

Optical sensors have demonstrated great potential as powerful analyte detection tools with low detection limits, high sensitivity, and fast response time.[1−3] In optical sensing, events are detected by changes in signals generated by fractional perturbations of the optical mode. An analyte with a refractive index different from that of its environment can therefore be detected in its natural form without labeling.[4−6] For biomolecular sensing, ligands are usually immobilized on a solid substrate of the sensing device to capture the target biomolecular in the inflowed fluid.[7,8] The captured biomolecules perturb the optical mode and generate a change in transduction signals, such as a resonance peak shift.

In real-time detection, the association phase can be detected based on the interactions between the biomolecular and ligand. These can be analyzed using the Langmuir adsorption model to reveal molecular dynamics such as association and dissociation rates.[4,9−13] To measure the concentration of the target biomolecule in the specimen, the initial slope of the association phase has to be obtained and compared with that of a reference sample whose concentration is already known.[14−16] However, when the fluid with the biomolecule reaches the device at the start of the reaction progression, the refractive index around the device is changed from that of the air to that of the fluid of the sample. This changes the optical path, and further beam alignment is required. During this alignment it is difficult to measure changes in the signal especially for the initial stages of the response. In addition, measuring a complete association phase to determine biomolecular concentrations by fitting the curve with the Langmuir equation is quite time-consuming. Instead, for practical applications, an effective method of measuring the concentration of the target analyte more quickly is needed, to avoid having to measure the signal completely from the starting point.

In this study, we propose a new practical method that is generally applicable to all types of affinity-based sensors as well as optical affinity sensors such as whispering gallery mode (WGM) or plasmonic sensors. By analyzing the fraction bound equation of the Langmuir adsorption model, we found that the ratio of fraction bound signal approaches the concentration ratio within the error range determined by the sample concentration and a dissociation constant. In this method, by comparing the fraction bound signal with that of a reference sample, the biomolecule concentration can be determined with a single measurement at any point in time. In addition, the proposed method is derived from a general equation that follows the Langmuir adsorption model, so it can be applied regardless of the type of biomolecules, such as nucleic acid and protein.

Received: February 13, 2020
Accepted: April 16, 2020
Published: April 16, 2020

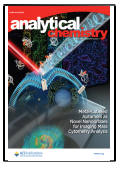

https://dx.doi.org/10.1021/acs.analchem.0c00637
Anal. Chem. 2020, 92, 6189−6193

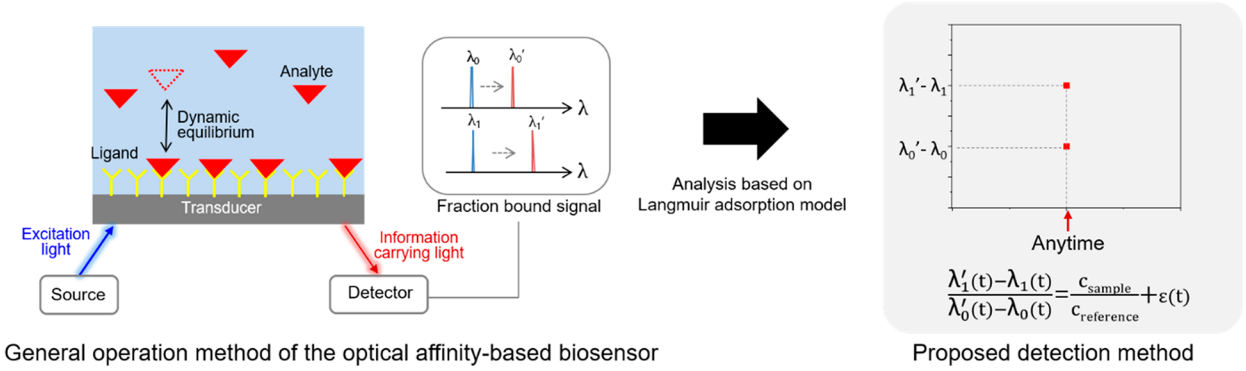

Figure 1. Concept illustration of the general operation method of the optical affinity-based biosensors and a proposed detection method for quick measurement of biomolecules concentration. In the affinity-based biosensor, the change in transducer signal such as resonance peak shifts caused by the interaction of targets with ligands can be measured. In this study, we found that the ratio of this change approaches the concentration ratio within the error range as shown in the equation of Figure 1. Based on this approach, we propose a new detection method that can determine the biomolecular concentration by single measurement at any point in time compared to the change of the reference sample.

Our method is similar to the concept of a balanced detection method that detects a small difference between two optical input signals, while greatly suppressing the general fluctuation of the input.[17,18] The proposed method also can suppress signal fluctuation of detectors evenly induced by external perturbations through simultaneous measurements, allowing more accurate measurement. We provide the theoretical maximum error rate of the proposed method, which is the largest error rate that can occur between the measured value and the actual concentration. It allows the measurement to be designed with a certain accuracy in advance. Finally, we experimentally demonstrated the proposed method and confirmed its accuracy by detecting a streptavidin and biotin complex using an on-chip optical sensor based on the active disk resonators integrated with a microfluidic channel.

METHOD

The association phase attained from the real-time measurement of affinity-based biosensors can be understood using the Langmuir adsorption model, which has been commonly used to analyze the kinetics of surface binding reactions for systems having a ligand immobilized on a solid surface, as shown in Figure 1.[8,11−13] Let A be a ligand and B be an analyte in solution which can form a bound product, AB.

$$A + B \leftrightarrow AB$$

The rate equations for the formation and the decay of the product AB are expressed as eq 1.

$$\frac{dc_{AB}}{dt} = k_{on}\cdot c_A\cdot c_B, \qquad \frac{dc_{AB}}{dt} = -k_{off}\cdot c_{AB} \tag{1}$$

(k_{on}, association rate; k_{off}, dissociation rate; c_A, c_B, c_{AB}, concentrations of A, B, and AB in a general solution)

In equilibrium, $\frac{dc_{AB}}{dt}$ is zero, and the association constant K_a and dissociation constant K_d are defined as,

$$K_a = \frac{1}{K_d} \equiv \frac{k_{on}}{k_{off}} = \frac{c_{AB}}{c_A\cdot c_B} \tag{2}$$

Based on the Langmuir adsorption model, the total analyte fixed on the substrate is constant.

$$n_{B,0} = n_B + n_{AB} = \text{constant} \tag{3}$$

In an affinity-based sensor, the $n_{B,0}$ and n_{AB} notations are used to emphasize that B and AB are attached to the transducer surface. The fraction bound in equilibrium, which is proportional to the transducer signal, is defined as the number of ligand and analyte complexes divided by the total number of ligands, as expressed in the equation below.

$$\text{fbeq}(c) \equiv \frac{n_{AB}}{n_{B,0}} = \frac{c}{c + K_d} \tag{4}$$

By solving eq 1 with eqs 2 and 3, the real-time association phase can be obtained, as expressed by the following eq 5.[8,11−13]

$$\text{fb}(t, c) = \alpha\cdot\text{fbeq}(c) \times [1 - \exp(-k_{on}^{obs}\cdot t)]$$
$$(k_{on}^{obs} = c\cdot k_{on} + k_{off}) \tag{5}$$

In eq 5, k_{on}^{obs} is an observable rate constant depending not only on c but also the intrinsic association rate k_{on} and dissociation rate k_{off}. Using the association phase in eq 5, we can define the intrinsic peak shift ratio $R(t)$:

$$R(t) \equiv \frac{\text{fb}(t, c_{sample})}{\text{fb}(t, c_{reference})} \tag{6}$$

The $R(t)$ is the ratio between the peak shifts of two different samples: one to be analyzed and the other for reference, where the concentration of analyte is already known. In the initial condition, $R(t)$ is

$$R(t) = R(0) = \frac{\text{fb}'(0, c_{sample})}{\text{fb}'(0, c_{reference})} = \frac{c_{sample}}{c_{reference}} \tag{7}$$

In this state, $R(t)$ can be reduced to the ratio of the original concentration. In the completely saturated state, $R(t)$ is

$$R(t) = R(\infty) = \frac{c_{sample}\cdot(c_{reference} + K_d)}{c_{reference}\cdot(c_{sample} + K_d)} \tag{8}$$

In the transient period, $R(t)$ has a value between the initial and saturated value because $R(t)$ is a monotonic function. Therefore, if the difference between the $R(t)$ and the actual concentration is defined as theoretical error $\varepsilon(t)$, the error rate of $R(t)$ from the ratio of the actual concentration can be expressed below.

https://dx.doi.org/10.1021/acs.analchem.0c00637
Anal. Chem. 2020, 92, 6189−6193

$$|\varepsilon(t)| \times \frac{c_{\text{reference}}}{c_{\text{sample}}} \times 100(\%)$$

The error rate is zero at the initial state and monotonically increases up to the maximum value, which occurs at the completely saturated state. Since the maximum error rate in this method is a function of the analyte concentration, the maximum error rate is plotted in Figure 2 for the normalized concentration of the sample and reference, which are defined as $\frac{C_{\text{sample}}}{K_d}$ and $\frac{C_{\text{reference}}}{K_d}$, respectively. In Figure 2, since the maximum error rate increases with the normalized concentration, we can determine the maximum concentration below which the unknown concentration can be measured with an accuracy better than a certain error rate.

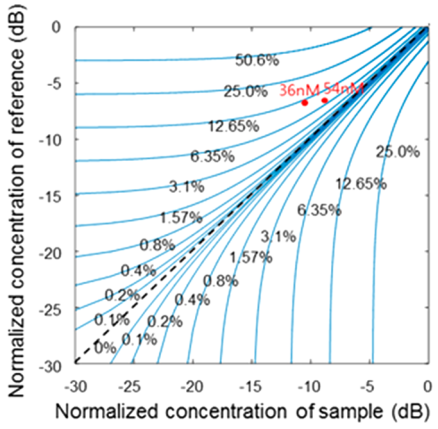

Figure 2. Blue contour lines represent the maximum error rate for the normalized concentration of the sample and reference. The value corresponding to each line is indicated. The black dashed line represents the zero error rate line, and the two red points indicate the maximum error rate of the 36 nM and 54 nM analytes used in the experiment with a 90 nM reference sample.

For example, if the normalized concentration of the reference is fixed to 10% of K_d, an unknown analyte concentration of less than 22.2% of K_d can be measured with an accuracy of less than a 10% error rate by a single measurement performed at any point in time. As a result, we prove that the concentration of the analyte is determined below a certain error rate by measuring the relative peak shift compared to the reference. In the case of $c_{\text{sample}}, c_{\text{reference}} \ll K_d$, the concentration rate converges to $R(t)$ at any time point.

Also, the proposed method can suppress signal fluctuations in the detector that are uniformly induced by external perturbation. When measuring concentration B, if the error is α, then the single measurement error rate is

$$\frac{|B + \alpha - B|}{B} = \frac{|\alpha|}{B} \tag{9}$$

When estimating the concentration of concentration B through peak shift ratio measurement, the error rate is

$$\frac{\left|\frac{B+\alpha}{A+\alpha}\cdot A - B\right|}{B} = \frac{\left|\alpha - \frac{B}{A}\cdot\alpha\right|}{B} \quad (A > \alpha) \tag{10}$$

The error rates of the above two measurement methods are compared as follows.

$$\frac{\frac{\left|\alpha - \frac{B}{A}\cdot\alpha\right|}{B}}{\frac{|\alpha|}{B}} = \left|1 - \frac{B}{A}\right| < 1 \quad (\text{when A} > \text{B}) \tag{11}$$

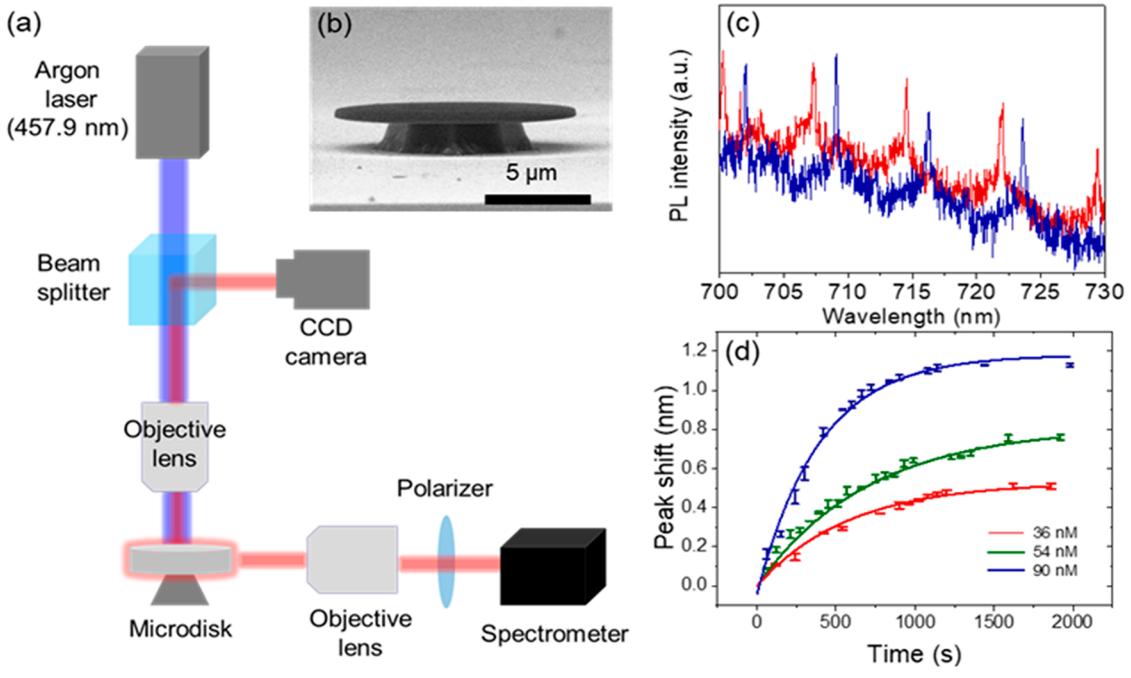

Figure 3. Experimental setup and peak shift measurement results. (a) Schematic of the experimental setup. (b) Scanning electron microscope image of the SRSN disk resonator. (c) PL spectrum of biotinylated SRSN disk resonator before (red line) and after (blue line) interaction with streptavidin in an aqueous environment. (d) Real-time peak shift of the resonance wavelength due to the binding of different concentrations of streptavidin to biotin on the resonator surface (point). This peak shift is fitted by the fraction bound equation of the Langmuir adsorption model. The error bars mean the standard deviation of the peak shift for the three fundamental modes.

https://dx.doi.org/10.1021/acs.analchem.0c00637
Anal. Chem. 2020, 92, 6189−6193

The proposed method allows the reference sample to be set at a value greater than the concentration of the sample to be measured. As a result, the error rate obtained using the ratio measurement is smaller than the single measurement error rate. This means that by combining the proposed method with the simultaneous measurement scheme, the fluctuation can be automatically suppressed out as a noise-canceling operation in the balanced detection.

EXPERIMENTAL RESULTS AND DISCUSSION

To experimentally demonstrate the proposed method, we developed on-chip optical biosensors based on an SRSN (silicon-rich silicon nitride) microcavity. The experiment setup is illustrated in Figure 3a, and the microcavity used in this experiment is shown in Figure 3b. Because of the large absorption cross-section of the silicon nanoclusters embedded in the SRSN disk plate, pump light illumination from the top of the resonator is enough to induce photoluminescence emission spectrum peaks along with resonance modes of the SRSN resonator. The photoluminescence emissions from the resonator are collected by an objective lens. This signal is detected by a charge-coupled detector (CCD) and spectrometer (Acton sp2500) via free-space optics. More details on the device design and experiment can be found in a previous work.[4]

The photoluminescence emission spectrum displays fundamental TM modes as shown in Figure 3c. We can attain the full width at half-maximum (FWHM) and resonance wavelength (λ_r) by performing a Lorentzian fitting of this mode. The quality factor (Q-factor) of the fundamental TM mode calculated from this spectrum is 8520. For the real-time detection of streptavidin, the device was prefunctionalized with biotin and integrated with a PDMS (polydimethylsiloxane) microfluidic channel. Streptavidin in DPBS (Dulbecco's phosphate-buffered saline) flows into the device through the microfluidic channel, interacting with the biotin fixed on the device surface, and it causes the resonance peak shifts to be detected. In Figure 3c, the red line is the photoluminescence spectrum without streptavidin, and the blue line is with streptavidin. The real-time peak shift for each concentration of streptavidin is shown in Figure 3d. The demonstrated sensitivity of the sensor is 0.012 nm/nM. The limit of detection (LOD) defined by the sensitivity and the resolution limit of the spectrometer, 0.05 nm, is 4.16 nM which is worse than the LOD in state-of-the-art studies.[2,5,19−21] However, this LOD is sufficient to verify the proposed balanced detection method by measuring the peak shift caused by the streptavidin−biotin interaction.

To verify the proposed method, a sample of 90 nM concentration was designated as the reference, and the 36 nM and 54 nM samples were designated as analytes. The ratios of streptavidin concentrations are plotted as dashed lines, which correspond to 0.4 for 36 nM and 0.6 for 54 nM with the reference of 90 nM concentration, respectively. The green and light purple triangles in Figure 4 are the measured peak shift ratio from the data in Figure 3d, with each point located near the dashed lines where the concentration ratio is located. If the actual concentration ratio is R and the measured peak shift ratio is $r(t)$, the average error rate can be calculated by $\sqrt{E(R - r(t))^2}$. The calculated average error rate of the measurement point, with the actual concentration ratio, are 9.0% and 9.5%, respectively.

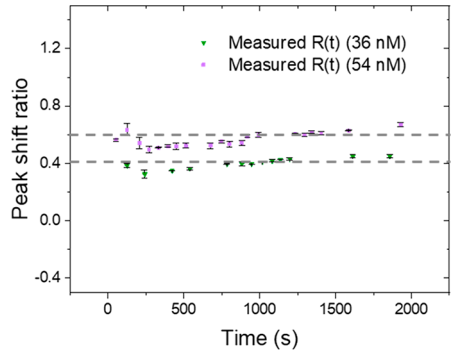

Figure 4. Ratios of the real-time resonance peak shift. The dashed lines represent the ratio of streptavidin concentration of 36 nM and 54 nM with a reference concentration of 90 nM, respectively. The error bars mean the standard deviation of peak shift ratio for the three fundamental modes.

In the initial measurement period, there are relatively larger deviations between the measurement and intrinsic peak shift ratios because of the inaccuracy of the peak shift measurement, mainly caused by a quantized error introduced by the 0.05 nm resolution limit of the spectrometer. In addition, the calculated maximum error rates for the samples (36 nM, 54 nM, and 90 nM) used in this experiment were 11% and 7.2%, the points indicated by the red dots in Figure 2. On the other hand, the concentration calculated through the initial slope of the association phase, which is a conventional method, was calculated to be 43 nM and 107.2 nM, with error rates of approximately 20% and 19%, respectively, for the actual concentration.[15,16]

The proposed method can be applied to all affinity-based sensors that follow the Langmuir adsorption model, regardless of biomolecule type or binding strength. For further verification, we applied our method to the binding kinetics sensorgram results in two previously published studies for DNA−DNA[23] and interleukin−gamma c interaction.[22] Figure 5a,c shows the original experimental data digitized from ref 22 and ref 23, respectively. As shown in Figure 5b,d, it was confirmed that the peak shift ratio coincides with the concentration ratio. The average error between the peak shift ratio and the concentration ratio was confirmed to be 15.2% for IL-7R 0.25 μM and 5.9% for IL-7R 1 μM and 13% for DNA 200 nM and 10% for the DNA 1000 nM. It is noteworthy that the detection experiments in the references were performed with commercial surface plasmon resonance (SPR) sensors instead of WGM sensors, which we used.

CONCLUSION

In this study, we proposed a real-time and quick method for measuring biomolecule concentration using a single measurement at any point in time. Since the method is derived from the fraction bound equation of the Langmuir adsorption model, which is not limited to optical sensors, it can be applied to all kinds of affinity-based sensors including electrochemical and electroacoustic devices. In addition, in principle, it is also applicable to any type of biomolecule, if following the Langmuir adsorption model.

We experimentally demonstrated and verified the proposed method through real-time measurement of signals induced by streptavidin−biotin interactions using an on-chip optical sensor integrated with a microfluidic channel. By combining

https://dx.doi.org/10.1021/acs.analchem.0c00637
Anal. Chem. 2020, 92, 6189−6193

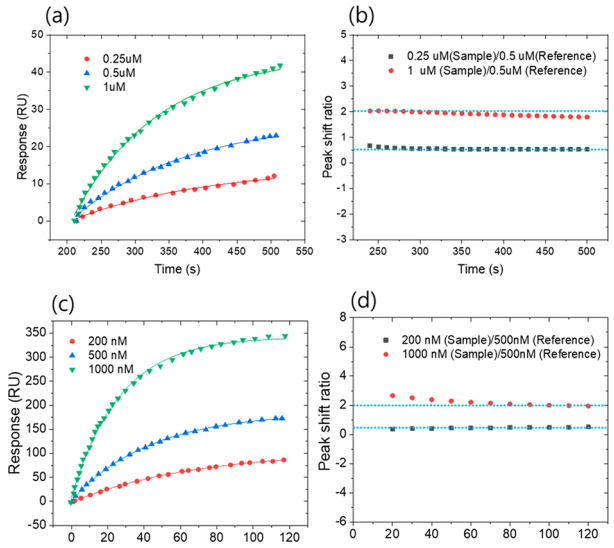

Figure 5. Application of the proposed method to other types of biomolecules. (a) Binding kinetic sensorgram results of the association of gamma c with IL-7R measured by SPR biosensor from ref 19. (b) The ratios of the real-time resonance peak shift. The blue lines represent the ratio of protein concentration with a reference concentration. (c) Binding kinetic sensorgram of DNA−DNA interaction between immobilized dG(TGGAA)2G and the ligand dC(TGGAA)2C at various ligand concentrations measured by SPR biosensor from ref 23. (d) The ratios of the real-time resonance peak shift. The blue lines represent the ratio of DNA concentration with a reference concentration.

the proposed method with a simultaneous measurement scheme, fluctuations in the transducer signal induced by external factors which influence both transducers evenly, such as temperature variation or surface pretreatment conditions, can be automatically suppressed out in the noise-canceling operation of balanced detection. We expect that our approach can be applied to practical applications such as clinical research that require a fast and accurate response.

AUTHOR INFORMATION

Corresponding Author

Hansuek Lee − *Department of Physics and Graduate School of Nanoscience and Technology, Korea Advanced Institute of Science and Technology, Daejeon 34141, Republic of Korea;* orcid.org/0000-0002-0748-7662; Email: hansuek@kaist.ac.kr

Author

Yeseul Kim − *Department of Physics, Korea Advanced Institute of Science and Technology, Daejeon 34141, Republic of Korea*

Complete contact information is available at: https://pubs.acs.org/10.1021/acs.analchem.0c00637

Author Contributions

Y.K. and H.L. created the concept and analytical method. The experiments were conceived, designed, and planned by Y.K. and H.L. The experiments were performed by Y.K. The manuscript was written by Y.K. and H.L.

Notes

The authors declare no competing financial interest.

ACKNOWLEDGMENTS

This work was supported by the National Research Foundation of Korea (NRF) grant funded by the Korea government (MSIT) (Grant 2020R1A2C1008292 and 2020R1A4A2002828). Thanks to Scott T. R. Walsh, Ming-Hon Hou, and I-Ren Lee for allowing us to use the data in Figure 5a,c.

REFERENCES

(1) Kim, E.; Baaske, M. D.; Vollmer, F. *Lab Chip* **2017**, *17*, 1190−1205.
(2) Baaske, M. D.; Foreman, M. R.; Vollmer, F. *Nat. Nanotechnol.* **2014**, *9*, 933−939.
(3) Vollmer, F.; Arnold, S. *Nat. Methods* **2008**, *5*, 591−596.
(4) Kim, Y.; Lee, H. *Opt. Express* **2019**, *27*, 34405−34415.
(5) Lu, T.; Lee, H.; Chen, T.; Herchak, S.; Kim, J. H.; Fraser, S. E.; Flagan, R. C.; Vahala, K. *Proc. Natl. Acad. Sci. U. S. A.* **2011**, *108*, 5976−5979.
(6) Zhu, J.; Ozdemir, S. K.; Xiao, Y.-F.; Li, L.; He, L.; Chen, D.-R.; Yang, L. *Nat. Photonics* **2010**, *4*, 46−49.
(7) Fan, X.; White, I. M.; Shopova, S. I.; Zhu, H.; Suter, J. D.; Sun, Y. *Anal. Chim. Acta* **2008**, *620*, 8−26.
(8) Lowe, B. M.; Sun, K.; Zeimpekis, I.; Skylaris, C. K.; Green, N. G. *Analyst* **2017**, *142*, 4173−4200.
(9) Yavas, O.; Svedendahl, M.; Dobosz, P.; Sanz, V.; Quidant, R. *Nano Lett.* **2017**, *17*, 4421−4426.
(10) Washburn, A. L.; Bailey, R. C. *Analyst* **2011**, *136*, 227−236.
(11) Halperin, A.; Buhot, A.; Zhulina, E. B. *J. Phys.: Condens. Matter* **2006**, *18*, S463−S490.
(12) Hanaor, D. A.; Ghadiri, M.; Chrzanowski, W.; Gan, Y. *Langmuir* **2014**, *30*, 15143−15152.
(13) Latour, R. A. *J. Biomed. Mater. Res., Part A* **2015**, *103*, 949−958.
(14) Washburn, A. L.; Gunn, L. C.; Bailey, R. C. *Anal. Chem.* **2009**, *81*, 9499−9506.
(15) Wildgen, S. M.; Dunn, R. C. *Biosensors* **2015**, *5*, 118−130.
(16) Eddowes, M. J. *Biosensors* **1987**, *3*, 1−15.
(17) Goobar, E. *IEEE J. Quantum Electron.* **1993**, *29*, 1116−1130.
(18) Houser, G. D.; Garmire, E. *Appl. Opt.* **1994**, *33*, 1059−1062.
(19) Degardin, K.; Desponds, A.; Roggo, Y. *Forensic Sci. Int.* **2017**, *278*, 313−325.
(20) Miotke, L.; Barducci, M.; Astakhova, K. *Chemosensors* **2015**, *3*, 224−240.
(21) Gao, F.; Lei, J.; Ju, H. *Anal. Chem.* **2013**, *85*, 11788−11793.
(22) McElroy, C. A.; Holland, P. J.; Zhao, P.; Lim, J. M.; Wells, L.; Eisenstein, E.; Walsh, S. T. *Proc. Natl. Acad. Sci. U. S. A.* **2012**, *109*, 2503−2508.
(23) Huang, T. Y.; Chang, C. K.; Kao, Y. F.; Chin, C. H.; Ni, C. W.; Hsu, H. Y.; Hu, N. J.; Hsieh, L. C.; Chou, S. H.; Lee, I. R.; Hou, M. H. *Proc. Natl. Acad. Sci. U. S. A.* **2017**, *114*, 9535−9540.

https://dx.doi.org/10.1021/acs.analchem.0c00637
Anal. Chem. 2020, 92, 6189−6193